Original paper

New ^{125}I brachytherapy source IsoSeed I25.S17plus: Monte Carlo dosimetry simulation and comparison to sources of similar design

Evaggelos Pantelis, PhD[1], Panagiotis Papagiannis, PhD[1], Giorgos Anagnostopoulos, PhD[2], Dimos Baltas, PhD[3]

[1]Medical Physics Laboratory, Medical School, University of Athens, Greece, [2]Pi Medical Ltd, Athens, Greece, [3]Department of Medical Physics & Engineering, Sana Klinikum Offenbach, Offenbach, Germany

Abstract

Purpose: To determine the relative dose rate distribution around the new ^{125}I brachytherapy source IsoSeed I25.S17plus and report results in a form suitable for clinical use. Results for the new source are also compared to corresponding results for other commercially available ^{125}I sources of similar design.

Material and methods: Monte Carlo simulations were performed using the MCNP5 v.1.6 general purpose code. The model of the new source was prepared from information provided by the manufacturer and verified by imaging a sample of ten non-radioactive sources. Corresponding simulations were also performed for the 6711 ^{125}I brachytherapy source, using updated geometric information presented recently in the literature. The uncertainty of the dose distribution around the new source, as well as the dosimetric quantities derived from it according to the Task Group 43 formalism, were determined from the standard error of the mean of simulations for a sample of fifty source models. These source models were prepared by randomly selecting values of geometric parameters from uniform distributions defined by manufacturer stated tolerances.

Results and Conclusions: Results are presented in the form of the quantities defined in the update of the Task Group 43 report, as well as a relative dose rate table in Cartesian coordinates. The dose rate distribution of the new source is comparable to that of sources of similar design (IsoSeed I25.S17, Oncoseed 6711, SelectSeed 130.002, Advantage IAI-125A, I-Seed AgX100, Thinseed 9011). Noticeable differences were observed only for the IsoSeed I25.S06 and Best 2301 sources.

J Contemp Brachytherapy 2013; 5, 4: 240–249
DOI: 10.5114/jcb.2013.39631

Key words: dosimetry, ^{125}I, Monte Carlo, TG43.

Purpose

The line of ^{125}I sources manufactured by Eckert & Ziegler BEBIG (Berlin, Germany) under the brand name IsoSeed, includes models I25.S06 with a gold radio-opaque marker [1], and I25.S17 with a molybdenum radio-opaque marker [2]. A variant of the latter model, IsoSeed I25.S17plus, has been designed to essentially replace the molybdenum marker with a silver one.

This work presents relative dosimetry data that is necessary for treatment planning in clinical applications employing the new source. This dataset was obtained by Monte Carlo (MC) simulations, adhering to the methodology recommendations in the update of the AAPM TG43 report (TG43-U1) [3]. Since these recommendations include, inter alia the reproduction of previously published dose distributions for at least one widely used source, simulations were also performed for the 6711 source [4-7]. Besides being similar in design to the I25.S17plus, the 6711 was chosen on the basis of newfound interest for its dosimetry, fueled by updated information on its geometry [4], and representing it as perhaps the best studied ^{125}I source in the literature.

Results of this work are also compared to corresponding results in the literature for other ^{125}I sources of design comparable to that of the new I25.S17plus.

Material and methods

Source characteristics

Information provided by the manufacturer, in the form of computer aided design files for the geometry of the IsoSeed I25.S17plus, the nominal dimensions, and the corresponding tolerances are presented in Fig. 1. The new source features the typical configuration of a cylin-

Address for correspondence: Panagiotis Papagiannis, PhD, Medical Physics Laboratory, Medical School, National and Kapodestrian University of Athens, 75 Mikras Asias St, Goudi – 115 27, Athens, Greece, phone: +30 210 746 2442, ✉ e-mail: ppapagi@phys.uoa.gr

Received: 13.10.2013
Accepted: 03.12.2013
Published: 31.12.2013

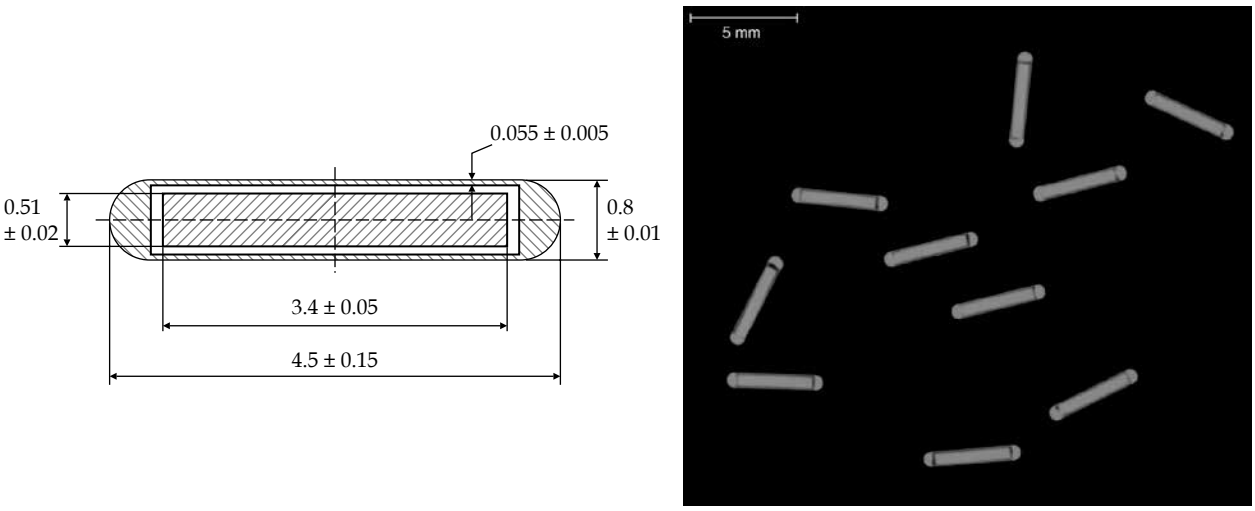

Fig. 1. Left: I25.S17plus source geometry, nominal dimensions and tolerances provided by the manufacturer. All dimensions are in mm. The marker's radioactive coating (not shown) is AgI (ρ = 5.675 g/cm^3) of 1 µm nominal thickness (± 30%). End weld thickness tolerance (not shown) is 0.35-0.40 mm. Right: Digital radiograph of 10 non-radioactive I25.S17plus sources

drical, high-Z, radio-opaque marker coated with 1 µm silver iodide containing radioactive ^{125}I, encapsulated in a hollow titanium cylinder (grade 2, % elemental composition: 0.015% H, 0.1% C, 0.03% N, 0.25% O, 0.2% Fe, 99.405% Ti), and sealed via laser welding of semi-spherical end caps.

The dimensions of the IsoSeed I25.S17plus were verified using high resolution digital radiography (see Fig. 1). An image of ten non-radioactive sources was obtained using magnification on a Senographe Essential mammography unit (GE Healthcare), operated at 22 kVp and 40 mAs. Measurements of the marker length (3.46 ± 0.05 mm), marker diameter (0.47 ± 0.06 mm), source length (4.40 ± 0.05 mm), source outer diameter (0.78 ± 0.06 mm), and end-weld thickness (0.41 ± 0.04 mm) were found to agree with nominal values within the absolute uncertainties of the latter. The source marker was found to present limited mobility in the encapsulation, as expected from the nominal dimensions of the source. Instances of concave or convex end welds were observed in the radiograph, in accordance with findings in the literature for other ^{125}I sources [4,6].

Besides small differences that in view of the physics underlying the low energy regime of ^{125}I photon emissions render every source design unique in terms of dosimetry, the new IsoSeed I25.S17plus design is comparable to that of the OncoSeed 6711 [4,6], SelectSeed 130.002 [8], Advantage IAI-125A [7], I-Seed AgX100 [9], and ThinSeed 9011 [5,6] sources. It is also comparable to its predecessors in the IsoSeed series, I25.S17 [2] and I25.S06 [1], as well as Best 2301 [7], with the exception of marker material which is Molybdenum, Gold and Tungsten, respectively, instead of silver.

For details on the design of the aforementioned ^{125}I sources, the interested reader should refer to the cited publications, or the publicly accessible TG43 Parameter databases of ESTRO (www.estro.org/about/governance-organisation/committees-activities/tg43-i-125) and the Carleton Laboratory for Radiotherapy Physics [7].

Monte Carlo simulation

All MC simulations of this work were performed using the MCNP5 v.1.6 general purpose MC radiation transport code [10]. The mcplib04 photoatomic cross-section library was used, which is based on the Lawrence Livermore National Laboratory (Livermore, CA) evaluated photon data library (1997 version). The ^{125}I energy spectrum was taken from the TG43-U1 report [3]. The MCNP standard model was employed, which includes incoherent scattering corrected for electron binding by means of the incoherent scattering factor, coherent scattering derived by applying the atomic form factor to the Thompson cross section, and explicit simulation of characteristic X-ray emission after photoelectric absorption in medium- and high-atomic number media.

The I25.S17plus source model was prepared using nominal dimensions (see Fig. 1) and semispherical end welds of 0.8 mm diameter. The void space between the marker and the Ti encapsulation was simulated as moist air (40% humidity) using composition and density information available in TG43-U1 [3]. The source model was centered in a spherical (15 cm radius) water geometry (ρ = 0.998 g/cm^3) [3].

Dose was approximated by the collisional kerma, since charged particle equilibrium can be assumed to exist in water around the seed. Scoring was performed using the *FMESH4 tally, which overlays a cylindrical mesh over the simulated geometry and tallies the energy fluency in each voxel of the mesh. Cylindrical symmetry of the source was assumed, and a 2D away and along dose rate table in liquid water was obtained using a cylindrical mesh resolution of 0.1 mm in both the y-axis (the transverse source bisector measuring distance "away"), and z-axis (the longitudinal source axis measuring distance "along") for away and along distances up to 5 cm, and 1 mm in both axes for away and along distances from 5 cm to 10 cm. The photon energy cutoff was 1 keV. The tally output was modified by the corresponding water mass

energy absorption coefficients, taken from the XCOM compilation [11] to convert photon energy fluence to water kerma values. The number of initial photons simulated was 3×10^9 to comply with good MC practice recommendations [3] regarding statistical uncertainty (the mean relative error was 0.2% at distances under 5 cm, the maximum standard errors of the mean were < 2% at distances under 5 cm and < 10% in the entire cylindrical mesh).

The number of initial photons used in simulations for the determination of the source air kerma strength (S_K) was 1×10^9. Energy photons less than 5 keV were not allowed to emerge from the source, in order to eliminate the contribution of 4.5 keV titanium K-edge X-rays to S_K in accordance with the National Institute of Standards and Technology (NIST), and the Physikalisch-Technische Bundesanstalt (PTB) standards [3,12]. The MCNP *F4 tally was used to score energy fluence in vacuo at a distance of d = 100 cm. The tally output was modified by the corresponding air mass energy absorption coefficients calculated based on the XCOM compilation [11] to convert photon energy fluency to air kerma rate. A point detector approximation (0.5º half angle) and a detector resembling the geometry of the NIST primary standard based on the Wide-Angle Free-Air Chamber (WAFAC – 7.6º half angle) were used, and $S_{K,Point}$ and $S_{K,WAFAC}$ were calculated by the product of corresponding air kerma rate results by d^2. A separate simulation was also performed using a detector resembling the geometry of the PTB primary standard based on the Grossvolumen Extrapolationskammer (GROVEX – 9.5º half angle) [12].

The dose rate constant of the I25.S17plus source, Λ_{Point} and Λ_{WAFAC}, was calculated, as the ratio of dose rate in liquid water at the reference point (r_0 = 1 cm, θ_0 = 90º) ≡ (y = 1 cm, z = 0 cm) by $S_{K,Point}$ and $S_{K,WAFAC}$, respectively. Linear interpolations within the 2D away and along dose rate table in liquid water were performed to determine the radial dose function, 2D anisotropy function, and 1D anisotropy function according to the TG43-U1 [3].

Corresponding simulations and calculations were performed for a model of the 6711 source prepared according to the information provided in the literature [6].

Uncertainty estimation

The update of the AAPM TG43 report [3] recommends that investigators include rigorous uncertainty analyses, as well as the effects of source geometric uncertainties. However, few studies have gone beyond assessing uncertainty at a few indicative points around a source. The most complete treatment of the subject involved performing MC simulations for minimum and maximum values of various geometric parameters to estimate the relative geometric uncertainty of TG43 quantities owing to each parameter, which was then combined in quadrature with other sources of uncertainty to arrive at a total uncertainty estimation [4].

A different approach was used in this work. A computer program was written to generate technically feasible I25.S17plus source models by randomly selecting values of geometric parameters. The selection was performed from uniform distributions defined by the tolerances provided by the manufacturer and presented in Fig. 1. The internal dimensions of the encapsulation were kept constant. Encapsulation thickness was then chosen randomly. The end welds were modeled as hemispheres of radius equal to the result for the outer radius of the encapsulation. However, their center was chosen randomly, so that their thickness varied within the corresponding tolerance. This procedure resulted to a random selection of the source length within ±0.1 mm of its nominal value (instead of its tolerance that is ±0.15 mm, see Fig. 1). The marker, diameter, length, and radioactive coating thickness were selected randomly, and marker movement was taken into account by randomly selecting its center position in the longitudinal direction. Marker movement in the transverse direction and marker tilt angle were not considered, since their contribution to uncertainty is expected to be insignificant for the I25.S17plus. The loss of cylindrical symmetry would lead to increased type A uncertainties of MC simulations described below.

Monte Carlo simulations were performed for a sample of 50 generated source models to obtain the relative dose rate distributions in water, as well as the corresponding air kerma strengths, $S_{K,WAFAC}$, as described in the previous section. The water dose rate distribution for each source model was normalized using its corresponding $S_{K,WAFAC}$. The average of the resultant normalized dose rate distributions should approach the nominal dose rate distribution for the IsoSeed I25.S17plus source, as this was found to be the case implying that the sample of 50 source models was adequate. The standard error of the mean at each point is a measure of nominal dose rate distribution relative uncertainty at that point, owing to geometric and type A uncertainties.

In order to estimate the total uncertainty of the nominal dose rate distribution for the IsoSeed I25.S17plus, values in the uncertainty matrix obtained as described above were combined in quadrature with 2% relative uncertainty in water cross sections [3,13], and 0.5% relative uncertainty in the water to air ratio of mass energy absorption coefficients in the energy range pertinent for this work [14]. This approach assumes that uncertainty due to volume averaging is negligible in view of the scoring grid resolution used in this work, and that a compensation error exists in the photon yield which cancels out in the normalization of water dose rate distributions with air kerma strength.

The complete characterization of nominal dose rate distribution uncertainty for the source also facilitates computing uncertainties of the TG43 dosimetric quantities at any point. This was performed using linear interpolation within the obtained uncertainty matrix, and uncertainty propagation along the lines of Medich *et al.* [15]. It should be noted that uncertainties for TG43 dosimetric quantities are provided in the following sections to facilitate comparisons with corresponding data. Since the TG43 quantities are not statistically independent, the uncertainty of dose rate calculations using them is not given by propagation of uncertainty; it is equal to the uncertainty of the nominal dose rate distribution used to derive them [15].

Results and Discussion

Away-along dose rate per unit air kerma strength results

Indicative dose rate per unit $S_{K,WAFAC}$ results for the new IsoSeed I25.S17plus source are given in Table 1, and plotted in Fig. 2A in the form of selected iso-dose-rate lines superimposed on a color map representation. These results were used for the derivation of TG43 quantities in the following, and they can be used for quality assurance purposes.

A color map representation of the relative uncertainty due to source geometry and type A uncertainties is given in Fig. 2B. Results are compatible with previous findings in the literature for the 6711 source [4], and it can be seen that geometric uncertainty is greatest at points lying at short distances and close to the longitudinal source axis, owing mainly to end weld thickness uncertainty. It should be noted that since MC results for each source model in the simulations for uncertainty estimation were normalized by their corresponding $S_{K,WAFAC}$ and not the

Table 1. Monte Carlo calculated dose rate per unit air kerma strength results ($cGyh^{-1}U^{-1}$) for the new IsoSeed I25.S17plus source. Total relative uncertainty (k = 1) is given in parentheses

	Distance away, y (cm)						
Distance along, z (cm)	0	0.25	0.5	1	2	4	6
0	–	14.3206 (2.1%)	3.8632 (2.1%)	0.9246 (2.1%)	0.1895 (2.1%)	0.0281 (2.1%)	0.0070 (2.1%)
0.25	–	8.7949 (3.5%)	3.2705 (2.4%)	0.8984 (2.1%)	0.1908 (2.1%)	0.0284 (2.1%)	0.0070 (2.1%)
0.5	0.9365 (3.0%)	2.6931 (3.2%)	1.9043 (2.2%)	0.7481 (2.1%)	0.1814 (2.1%)	0.0281 (2.1%)	0.0070 (2.1%)
1	0.2775 (3.1%)	0.5389 (3.2%)	0.5932 (2.4%)	0.4098 (2.1%)	0.1453 (2.2%)	0.0262 (2.1%)	0.0068 (2.1%)
2	0.0778 (2.8%)	0.1034 (3.1%)	0.1178 (2.6%)	0.1184 (2.2%)	0.0732 (2.1%)	0.0197 (2.1%)	0.0058 (2.1%)
3	0.0316 (3.3%)	0.0378 (3.0%)	0.0403 (2.6%)	0.0430 (2.3%)	0.0343 (2.1%)	0.0132 (2.1%)	0.0045 (2.2%)
4	0.0134 (3.1%)	0.0173 (2.9%)	0.0172 (2.6%)	0.0185 (2.3%)	0.0166 (2.1%)	0.0083 (2.1%)	0.0033 (2.1%)
5	0.0081 (3.6%)	0.0089 (3.1%)	0.0085 (2.8%)	0.0089 (2.4%)	0.0085 (2.2%)	0.0050 (2.1%)	0.0023 (2.1%)
6	0.0042 (3.3%)	0.0047 (2.6%)	0.0045 (2.5%)	0.0046 (2.4%)	0.0045 (2.2%)	0.0030 (2.1%)	0.0016 (2.1%)
7	0.0023 (3.7%)	0.0026 (2.7%)	0.0025 (2.6%)	0.0025 (2.4%)	0.0025 (2.2%)	0.0018 (2.1%)	0.0010 (2.1%)
8	0.0012 (3.0%)	0.0015 (2.5%)	0.0015 (2.6%)	0.0015 (2.5%)	0.0014 (2.3%)	0.0011 (2.1%)	0.0007 (2.1%)
9	0.0008 (3.5%)	0.0009 (2.6%)	0.0009 (2.5%)	0.0009 (2.4%)	0.0008 (2.2%)	0.0007 (2.1%)	0.0004 (2.1%)
10	0.0004 (4.8%)	0.0005 (3.1%)	0.0005 (2.5%)	0.0005 (2.4%)	0.0005 (2.3%)	0.0004 (2.2%)	0.0003 (2.1%)

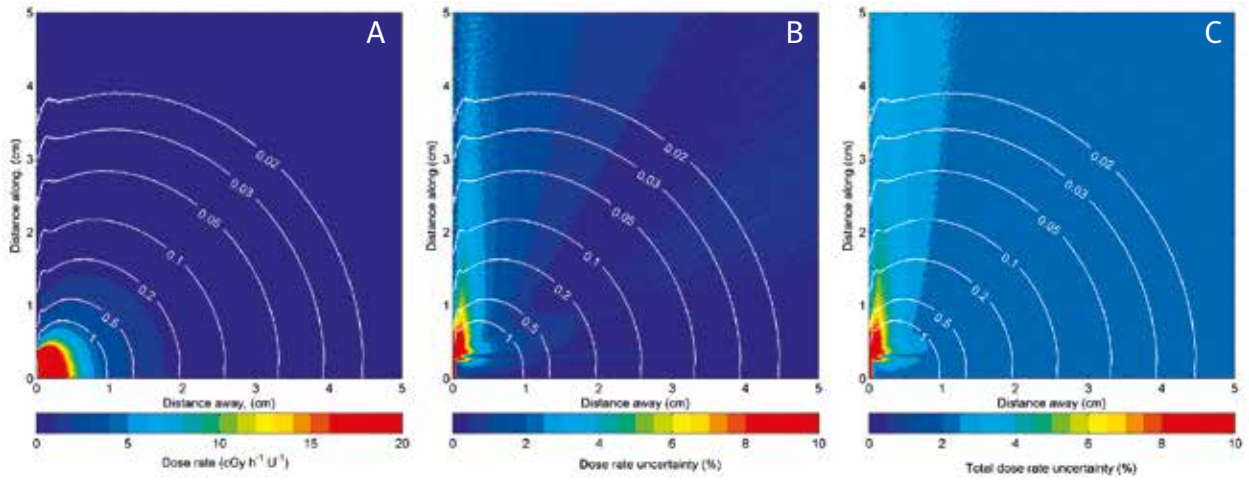

Fig. 2. A) A color map representation of dose rate versus distance along and away from the new I25.S17plus source. B) Relative uncertainty of dose rate results in (A) due to source geometrical uncertainty and MC simulation type A uncertainty. C) Total relative uncertainty of dose rate results in (A) obtained from the quadrature combination of relative uncertainty in (B) with cross sections and water to air mass energy absorption ratio uncertainties. Selected isodose rate lines (in units of $cGyh^{-1}U^{-1}$) are superimposed in all figures

nominal one, presented results correspond to the best practice scenario of individual source calibration [16]. If this is not the case, an additional uncertainty component of 1.23% has to be combined in quadrature. This is due to the effect of geometric uncertainty to $S_{K,WAFAC}$ (2.494 × 10^{-8} $MeVg^{-1}$ for the nominal source model) that was

Table 2. Comparison of MC calculated dose rate constant results of this work for the new I25.S17plus and the 6711 sources, with corresponding MC and consensus results in the literature for ^{125}I sources of similar design. Please refer to the text for the explanation of methods

Model	Method	$\Lambda^{\dagger}$ ($cGyh^{-1}U^{-1}$)		Reference
IsoSeed I25.S17plus	Λ_{WAFAC}	0.925	(19)	This work
	Λ_{point}	0.946	(21)	
IsoSeed I25.S17	Λ_{WAFAC}	0.914	(5)	Lymperopoulou 2005 [2]
	Λ_{point}	0.944	(5)	
IsoSeed I25.S06	Consensus	1.012	(49)	TG43-U1 [3]
	Λ_{WAFAC}	0.991	(3)	Williamson 2002 [21]
	Λ_{point}	1.002	–	Hedtjarn 2000 [1]
Oncoseed 6711	Consensus	0.965	(46)	TG43-U1 [3]
	Λ_{WAFAC}	0.942	(17)	Dolan 2006 [4]
	Λ_{point}	0.942	(17)	Dolan 2006 [4]
	Λ_{WAFAC}	0.904	(21)	Rivard 2009 [5]
	Λ_{point}	0.929	(21)	
	Λ_{WAFAC}	0.921	(7)	Kennedy 2010 [6]
	Λ_{point}	0.939	(4)	
	Λ_{WAFAC}	0.924	(2)	Taylor and Rogers 2008 [7]
	Λ_{point}	0.942	(3)	
	Λ_{WAFAC}	0.932	(19)	This work
	Λ_{point}	0.941	(20)	
SelectSeed 130.002	Λ_{point}	0.954	(5)	Karaiskos 2001 [8]
	Λ_{WAFAC}	0.925	(5)	Lymperopoulou 2005 [2]
	Λ_{point}	0.950	(5)	
Advantage IAI-125A	Consensus	0.981	(47)	TG43-U1S1 [17]
	Λ_{WAFAC}	0.925	(2)	Taylor and Rogers 2008 [7]
	Λ_{point}	0.959	(2)	
Best 2301	Consensus	1.018	(49)	TG43-U1 [3]
	Λ_{WAFAC}	0.998	(2)	Taylor and Rogers 2008 [7]
	Λ_{point}	1.002	(3)	
I-Seed AgX100	Λ_{WAFAC}	0.918	(24)	Mourtada 2011 [9]
	Λ_{point}	0.943	(24)	
Thinseed 9011	Λ_{WAFAC}	0.914	(21)	Rivard 2009 [5]
	Λ_{point}	0.918	(21)	
	Λ_{WAFAC}	0.923	(4)	Kennedy 2010 [6]
	Λ_{point}	0.928	(4)	

MC – Monte Carlo, WAFAC – Wide Angle Free Air Chamber type A or combined standard uncertainty (k = 1), as appearing in the corresponding references and rounded up to the last significant digit of reported Λ, is given in parentheses

found to vary by 1.2% (standard error of the mean) in the simulations for uncertainty estimation.

Figure 2C presents the total uncertainty of dose rate results using the same color map as in Fig. 2B. Numerical data for relative uncertainty included in Table 1 were derived from the data set plotted in this figure. While these single source uncertainties are considerable, preliminary results for clinical prostate implants show that due to the increased number of implanted seeds, clinical dosimetry is affected less than 1% at the surface of the planning target volume and less than 2% within it [17].

Dose rate constant, Λ

The MC calculated dose rate constant proposed for clinical use with the IsoSeed I25.S17plus is Λ_{WAFAC} = (0.925 ± 0.019) cGyh^{-1}U^{-1}.

In Table 2, dose rate constant results of this work for the new IsoSeed I25.S17plus and the 6711 sources are summarized and compared to corresponding results in the literature for the 6711, as well as other ^{125}I sources of similar design. The method column in this table differentiates between consensus and MC calculations. The former are values proposed for clinical use, obtained by the equally weighted average of the separately averaged experimental and MC values in the literature [3,18]. They are presented merely for completeness, since experimental values determined using TLD-100 at that time were not corrected for a component of energy dependence related to the solid state of the detector that cannot be calculated using MC simulation [6,19,20]. If not accounted for, this energy dependence component leads to an overestimation of experimental results [6,20]. This explains why consensus values are systematically greater than MC results in Table 2, even if in most cases agreement with MC values is within their combined standard uncertainty which is considerable due to the propagation of experimental uncertainties.

Monte Carlo dose rate constant results in Table 2 correspond to normalization of dose rate in water by $S_{K,point}$ or $S_{K,WAFAC}$ (Λ_{point} and Λ_{WAFAC}, respectively). Λ_{point}, and Λ_{WAFAC} results should agree except for sources where the contribution of the radioactivity distribution at points along the transverse source bisector is partially obscured by sharp corners or edges of the radio-opaque marker. This is the case with the new I25.S17plus and sources of similar design included in Table 1, due to radioactivity distributed also on the edges of their cylindrical markers. This effect was originally reported by Williamson [21,22] and later discussed by Karaiskos *et al.* [8] to explain non-monotonic behavior of anisotropy function results for an ^{125}I source. Due to the polar angle volume averaging effect leading to increased air kerma strength, Λ_{WAFAC} results are expected to be smaller than Λ_{point} results. Since the magnitude of this effect depends on the ratio of marker diameter to marker length, differences between Λ_{WAFAC} and Λ_{point} results in Table 2 are negligible for the 2301, I25.S06 and 9011, and more pronounced for the rest of the sources, depending also on investigator and reaching up to 3.5%.

In any case, the Λ_{WAFAC} values should be considered for clinical use since they adhere to the current calibration standards and allow for direct comparison with experimental determinations using sources calibrated according to them [3]. While NIST and PTB calibrations have been found to agree within less than 1% [12], the polar angle volume averaging effect discussed above could be different in air kerma calibrations for the I25.S17plus and sources of similar design. Although the geometry of the primary standard instruments was not explicitly simulated in this work, the result for the I25.S17plus in the simulation using a detector with a half-angle equal to that of the GROVEX chamber was found 1% lower than $S_{K,WAFAC}$. However, this is well within the uncertainty (k = 2) of the NIST and PTB calibrations [12], and translates to a difference of the dose rate constant that is well within its associated uncertainty. Therefore, no differentiation is made between NIST and PTB calibrations in dosimetry results of this work for the I25.S17plus source (i.e. dose rate data in Table 1 and the Λ_{WAFAC} value in Table 2 can be used with sources whose calibration is traceable to either institute).

Table 3. Radial dose function results of this work for the new I25.S17plus and the 6711 sources. Total absolute uncertainty (k = 1) is given in parentheses

	$g_L(r)$		
r (cm)	I25.S17plus		6711
0.10	1.059	(32)	1.050
0.15	1.080	(32)	1.068
0.20	1.089	(32)	1.082
0.25	1.092	(32)	1.087
0.30	1.091	(32)	1.087
0.50	1.073	(31)	1.073
0.75	1.040	(30)	1.041
1.00	1.000	(–)	1.000
1.50	0.909	(27)	0.909
2.00	0.814	(24)	0.815
2.50	0.722	(21)	0.724
3.00	0.635	(19)	0.636
3.50	0.555	(16)	0.556
4.00	0.482	(14)	0.484
4.50	0.419	(12)	0.420
5.00	0.363	(11)	0.364
6.00	0.270	(8)	0.270
7.00	0.199	(6)	0.199
8.00	0.147	(4)	0.149
9.00	0.109	(3)	0.109
10.00	0.079	(2)	0.080

Focusing to 6711 results in Table 2, the outcome of this work agree within 1% with results presented in the literature, except for Rivard 2009 [5] where agreement is within 1.3% and 3.1% for Λ_{point}, and Λ_{WAFAC} results, respectively. This is probably due to the fact that silver was not included in the active layer composition in simulations of Rivard [5,6]. It is also worth noting that agreement is within type A uncertainty for Λ_{point} results since, due to its simplicity, this approach is less prone to methodological bias.

Finally, results in Table 2 indicate that the dose rate constant of the new I25.S17plus agrees within uncertainties with all presented sources with a silver marker (6711, 130.002, IAI-125A, AgX100, and 9011). Differences are observed only with the I25.S17 (1.2% for Λ_{WAFAC}), I25.S06 (7.2% for Λ_{WAFAC}), and 2301 (7.9% for Λ_{WAFAC}) sources, due to subtle differences in the emitted photon spectrum resulting from the contribution of characteristic x-ray emissions from their different marker materials.

Radial dose function, $g_L(r)$

Radial dose function results of this work for the 6711 source (presented in Table 3) are in excellent agreement with consensus values [3] based on Williamson [23] (better than 1% except for 3% at r = 4 cm), and results based on updated geometry information on the beveled source marker by Rivard [5] and Kennedy *et al*. [6] (better than 1%). A good agreement was also observed with results of

Table 4. 2D anisotropy function results of this work, F(r, θ), for the new I25.S17plus and the 6711 source. Total absolute uncertainty (k = 1) is given in parentheses

	F (0.25 cm θ)			F (0.5 cm θ)			F (1 cm θ)			F (2 cm θ)			F (3 cm θ)			F (5 cm θ)		
θ (degrees)	I25.S17plus		6711	I25.S17plus		6711	I25.S17plus		6711	I25.S17plus		6711	I25.S17plus		6711	I25.S17plus		6711
0	0.211	(42)	0.168	0.208	(10)	0.202	0.287	(16)	0.271	0.400	(16)	0.312	0.469	(19)	0.383	0.556	(22)	0.576
2	0.213	(42)	0.171	0.212	(11)	0.200	0.344	(14)	0.286	0.508	(20)	0.392	0.573	(21)	0.453	0.645	(23)	0.520
4	0.218	(40)	0.179	0.306	(18)	0.231	0.459	(22)	0.328	0.538	(22)	0.416	0.581	(21)	0.464	0.632	(19)	0.527
6	0.288	(50)	0.215	0.394	(26)	0.271	0.455	(22)	0.338	0.536	(20)	0.426	0.587	(21)	0.476	0.640	(22)	0.542
8	0.401	(64)	0.272	0.406	(27)	0.284	0.479	(22)	0.356	0.563	(20)	0.443	0.609	(21)	0.493	0.661	(22)	0.552
10	0.502	(76)	0.325	0.444	(29)	0.310	0.516	(22)	0.385	0.594	(21)	0.471	0.637	(21)	0.520	0.682	(22)	0.576
12	0.571	(83)	0.376	0.493	(30)	0.353	0.558	(23)	0.424	0.629	(22)	0.503	0.667	(22)	0.547	0.710	(22)	0.601
14	0.658	(85)	0.456	0.544	(31)	0.403	0.599	(24)	0.466	0.662	(22)	0.538	0.694	(22)	0.578	0.734	(23)	0.625
16	0.737	(84)	0.536	0.594	(32)	0.455	0.636	(24)	0.507	0.693	(23)	0.574	0.722	(23)	0.610	0.755	(24)	0.650
18	0.809	(81)	0.607	0.640	(32)	0.507	0.673	(25)	0.549	0.721	(23)	0.607	0.747	(23)	0.640	0.773	(24)	0.678
20	0.869	(78)	0.666	0.681	(33)	0.556	0.705	(25)	0.587	0.746	(24)	0.638	0.769	(24)	0.667	0.796	(24)	0.701
25	0.971	(72)	0.781	0.771	(33)	0.665	0.776	(26)	0.675	0.802	(25)	0.710	0.817	(25)	0.729	0.837	(25)	0.755
30	1.023	(70)	0.860	0.840	(32)	0.752	0.832	(26)	0.749	0.849	(26)	0.771	0.858	(26)	0.784	0.866	(26)	0.801
35	1.037	(66)	0.914	0.896	(31)	0.816	0.878	(27)	0.811	0.887	(26)	0.823	0.893	(26)	0.831	0.899	(27)	0.847
40	1.036	(52)	0.950	0.942	(31)	0.867	0.916	(27)	0.858	0.918	(27)	0.866	0.920	(27)	0.869	0.922	(27)	0.877
45	0.999	(34)	0.974	0.978	(32)	0.907	0.948	(28)	0.896	0.945	(28)	0.899	0.943	(28)	0.902	0.943	(28)	0.904
50	0.970	(42)	0.987	1.007	(33)	0.939	0.976	(29)	0.928	0.969	(29)	0.927	0.966	(29)	0.928	0.961	(29)	0.928
55	0.981	(43)	0.970	1.025	(34)	0.963	0.998	(29)	0.953	0.988	(29)	0.953	0.983	(29)	0.951	0.977	(29)	0.954
60	0.989	(39)	0.977	1.033	(34)	0.982	1.017	(30)	0.975	1.004	(30)	0.973	0.997	(30)	0.969	0.989	(29)	0.968
65	0.995	(36)	0.985	1.034	(33)	0.997	1.030	(31)	0.992	1.019	(30)	0.989	1.011	(30)	0.985	1.003	(30)	0.982
70	0.999	(33)	0.993	0.995	(30)	1.003	1.034	(31)	1.002	1.028	(30)	0.999	1.021	(30)	0.995	1.010	(30)	0.989
75	1.001	(32)	0.998	0.996	(31)	0.993	1.035	(30)	1.010	1.031	(30)	1.007	1.024	(30)	1.002	1.015	(30)	1.001
80	1.003	(30)	1.001	1.000	(30)	0.998	1.005	(30)	1.009	1.030	(30)	1.011	1.025	(30)	1.009	1.017	(30)	1.002
85	1.002	(30)	1.001	1.001	(29)	1.001	1.000	(29)	1.001	1.005	(30)	1.005	1.020	(30)	1.008	1.014	(30)	1.006
90	1.000	(–)	1.000	1.000	(–)	1.000	1.000	(–)	1.000	1.000	(–)	1.000	1.000	(–)	1.000	1.000	(–)	1.000

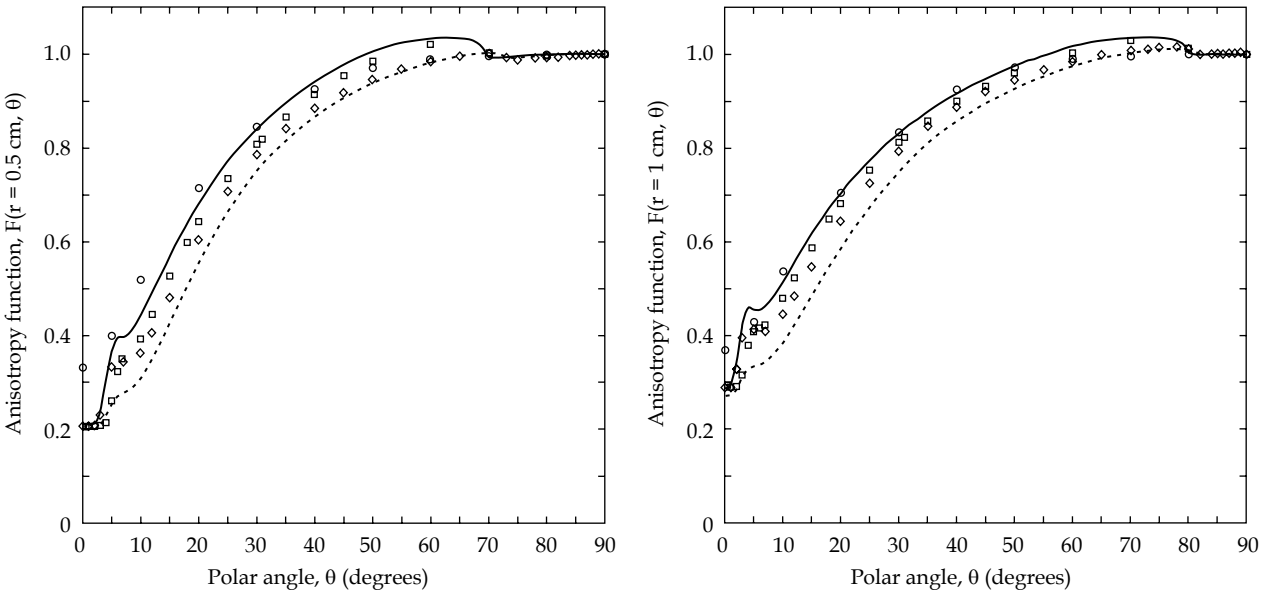

Fig. 3. Anisotropy function values of this work for the new I25.S17plus (solid line) and the 6711 source (broken line) plotted as a function of polar angle θ at radial distances r = 0.5 cm (left) and r = 1 cm (right). Corresponding results of Lymperopoulou *et al*. [2] for the I25.S17 source (□), and consensus data [3] (○) as well as results of Taylor and Rogers [7] (◊) for the 6711 source are also presented for comparison

Taylor and Rogers [7] (within 3%) and Dolan [4] (differences up to 4% except for 6% at r = 0.1 cm) with a trend of results of this work to be higher at distances < 1 cm and lower at large distances.

Results of this work for the new I25.S17plus source are also presented in Table 3. They were found in close agreement (within 2%) with corresponding MC results for the I25.S17 source which has a Molybdenum marker, as well as all silver marker sources considered in this work (6711, I25.S17 [2], AgX [9], 130.002 [8], 9011 [6], IAI-125A [7]). It is worth noting that while results of this work for the new I25.S17plus are in close agreement (better than 2%) with results of Taylor and Rogers [7] for the IAI-125A source, consensus data for the IAI-125A source [18] are greater up to 29% at large distances. Due to their different marker materials, the radial dose rate of the new I25.S17plus is 5% higher at small distances, and 23% and 30% lower at large distances relative to that of the I25.S06 [3] and 2301 [3] sources, respectively.

2D and 1D anisotropy function, F(r,θ) and $\varphi_{an}(r)$

F(r,θ) results of this work for the I25.S17plus and the 6711 source are presented in Table 4.

Due to its beveled marker ends [4], anisotropy results for the 6711 are expected to be lower than the consensus values [3]. Results of this work for the 6711 source however are lower than corresponding results in the literature especially at small polar angles. Results in the Carleton database [7] are higher by up to 31%, 21%, and 16% at 0.5 cm, 1 cm, and 5 cm, respectively (see also Fig. 3). Corresponding differences were observed in the comparison of results of this work with other MC data for source models prepared using updated geometric information presented recently in the literature [4-6].

Results of this work for the I25.S17plus are comparable to corresponding results in the literature for sources of similar design, especially at θ > 10° (see also Fig. 3). The new source appears to be less anisotropic (exhibits higher

Table 5. 1D anisotropy function results of this work, ϕan (r), for the new I25.S17plus and the 6711 source. Total absolute uncertainty (*k* = 1) is given in parentheses

	ϕ_{an} (r)		
r (cm)	I25.S17plus		6711
0.25	1.162	(24)	1.039
0.5	0.992	(20)	0.929
0.75	0.967	(20)	0.914
1	0.961	(20)	0.912
1.5	0.958	(20)	0.913
2	0.957	(20)	0.915
2.5	0.956	(20)	0.916
3	0.957	(20)	0.919
4	0.960	(20)	0.923
5	0.956	(20)	0.928
6	0.960	(20)	0.927
7	0.960	(20)	0.933
8	0.963	(20)	0.927
9	0.955	(20)	0.931

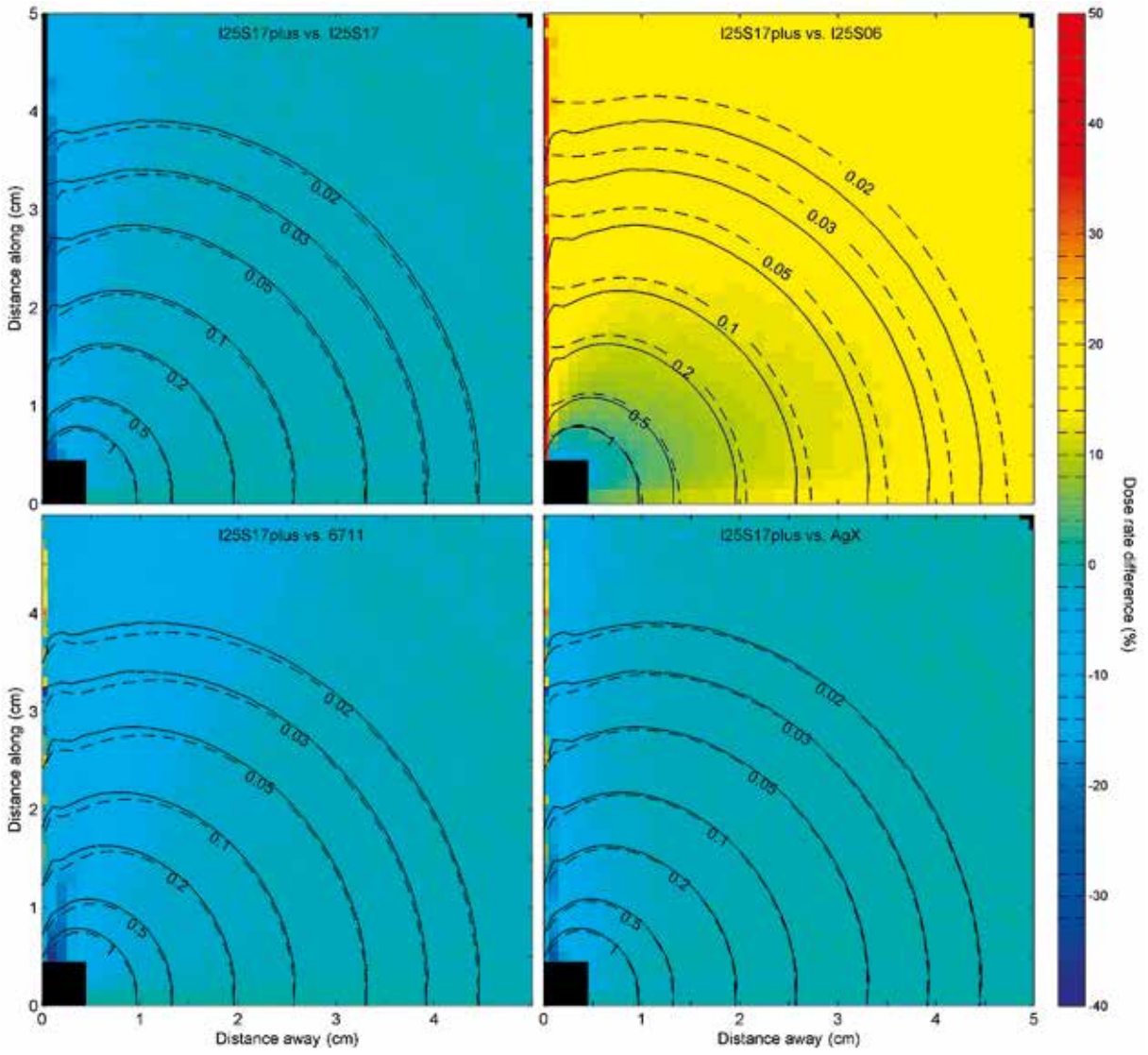

Fig. 4. Percentage differences between the dose rate distribution calculated in this work for the new I25.S17plus source and corresponding data for the I25.S17 [2], I25.S06 [3], 6711 [7] and AgX [9] sources, presented on a pixel by pixel basis using an appropriate colormap. Dose rate distributions sources other than the I25.S17plus were calculated using linear interpolation on published TG43 data. Results are not presented at pixels where extrapolations to data in the literature had to be performed. Selected isodose-rate lines (in units of $cGyh^{-1}U^{-1}$) are superimposed to facilitate the comparison. Solid lines correspond to the I25.S17plus and dashed lines correspond to the source compared to it in each subplot

anisotropy values, albeit within uncertainties in most of the cases) than the I25.S17 [2], 6711 [4,6], SelectSeed [8], IAI-125A [7], AgX100 [9], and ThinSeed 9011 [5,6] sources. It is however more anisotropic in its dose rate distribution relative to the I25.S06 [1], and Best 2301 [3] sources.

The $\varphi_{an}(r)$ results of this work for the I25.S17plus and the 6711 source, presented in Table 5, are in close agreement (4% maximum difference for $r > 0.5$ cm) with corresponding data for all sources of similar design considered in this work.

Comparison of the I25.S17plus and similar source designs in the form of dose rate distributions

The dosimetry comparison of the new I25.S17plus source and sources of similar design presented in the previous sections in the form of a comparison between corresponding results for TG43 quantities, can be summarized by a direct comparison of dose rate distributions on the central yz plane (the plane containing the source axis). Such a comparison between the dose rate distributions of the I25.S17plus and four selected sources of similar design is presented in Fig. 4.

This figure attests that the dose rate distribution of the I25.S17plus is comparable to that of sources of similar design and the same marker material such as the 6711 and the AgX. Increased differences are only observed at points close to the longitudinal source axis where subtle differences in the nominal source geometries matter the most, and uncertainty due to the tolerances in the source geometries is more pronounced (see also Fig. 1B). These

differences may also be partly attributed to the smoothing of dose rate distributions calculated for sources compared to the I25.S17plus in Fig. 4. This is due to the resolution of published data that is coarse compared to the original data sets, especially in view of the non-monotonic behavior of the anisotropy function close to the longitudinal axis. The dose rate distribution of the I25.S17plus is also comparable to that of the I25.S17 source besides their different marker materials (silver and molybdenum, respectively). On the contrary, Fig. 4 suggests that the I25.S06 source (gold marker) delivers greater dose than the I25.S17plus, especially at greater distances from the source.

Conclusions

Monte Carlo simulation was used to determine the dose rate distribution around the new IsoSeed I25.S17plus source and estimate its uncertainty. Dosimetric quantities defined in the update of the AAPM TG43 report [3] are provided, in partial fulfillment of the AAPM dosimetric prerequisites [24] for consensus data set preparation and inclusion of the source in the corresponding Joint AAPM/RPC Registry [25]. An experimental study of the source dosimetry is under way.

Comparison to other ^{125}I sources of similar design shows that the new source is dosimetrically equivalent to the I25.S17, 6711, 130.002, IAI-125A, AgX100, and 9011 sources, except at points close to the longitudinal source axis. Differences are more pronounced between the new source and the I25.S06 and 2301 sources.

Acknowledgements

Mr Michael Andrássy, Senior Physicist at Eckert & Ziegler BEBIG GmbH, is gratefully acknowledged for useful discussions and information on source geometry, as well as for arranging the delivery of a non-radioactive source batch. The authors thank Dr. Panagiotis Kipouros, Medical Physicist at "Helena Venizelou" General and Maternity Hospital for assistance in imaging the non-radioactive source batch.

References

1. Hedtjärn H, Carlsson GA, Williamson JF. Monte Carlo-aided dosimetry of the symmetra model I25.S06 ^{125}I, interstitial brachytherapy seed. *Med Phys* 2000; 27: 1076-1085.
2. Lymperopoulou G, Papagiannis P, Sakelliou L. Monte Carlo and thermoluminescence dosimetry of the new IsoSeed® model I25.S17 ^{125}I interstitial brachytherapy seed. *Med Phys* 2005; 32: 3313-3317.
3. Rivard MJ, Coursey BM, DeWerd L et al. Update of AAPM Task Group No. 43 Report: A revised AAPM protocol for brachytherapy dose calculations. *Med Phys* 2004; 31: 633-674.
4. Dolan J, Li Z, Williamson JF. Monte Carlo and experimental dosimetry of an ^{125}I brachytherapy seed. *Med Phys* 2006; 33: 4675-4684.
5. Rivard M. Monte Carlo radiation dose simulations and dosimetric comparison of the model 6711 and 9011 ^{125}I brachytherapy sources. *Med Phys* 2009; 36: 486-491.
6. Kennedy RM, Davis SD, Micka JA et al. Experimental and Monte Carlo determination of the TG-43 dosimetric parameters for the model 9011 THINSeed™ brachytherapy source. *Med Phys* 2010; 37: 1681-1688.
7. Taylor RE, Yegin G, Rogers DW. Benchmarking brachydose: Voxel based EGSnrc Monte Carlo calculations of TG-43 dosimetry parameters. *Med Phys* 2007; 34: 445-457.
8. Karaiskos P, Papagiannis P, Sakelliou L et al. Monte Carlo dosimetry of the selectSeed ^{125}I interstitial brachytherapy seed. *Med Phys* 2001; 28: 1753-1760.
9. Mourtada F, Mikell J, Ibbott G. Monte Carlo calculations of AAPM Task Group Report No. 43 dosimetry parameters for the ^{125}I I-Seed AgX100 source model. *Brachytherapy* 2011; 11: 237-244.
10. X-5 Monte Carlo Team, MCNP-A general Monte Carlo N-particle transport code, Version 5," Los Alamos National Laboratory Report No. LA-UR-03-1987, Los Alamos, NM, 2005.
11. J. Hubbell, M. Seltzer. Tables of x-ray mass attenuation coefficients and mass energy-absorption coefficients. NIST 1995. Available online at: http://physics.nist.gov/PhysRefData/XrayMassCoef/tab4.html.
12. Selbach HJ, Kramer HM, Culberson WS. Realization of reference air-kerma rate for low-energy photon sources. *Metrologia* 2008; 45: 422-428.
13. Hubbell JH. Review of photon interaction cross section data in the medical and biological context. *Phys Med Biol* 1999; 44: R1-R2.
14. Andreo P, Burns D T, Salvat F. On the uncertainties of photon mass energy-absorption coefficients and their ratios for radiation dosimetry. *Phys Med Biol* 2012; 57: 2117-2136.
15. Medich DC, Tries MA, Munro III JJ. Monte Carlo characterization of an ytterbium-169 high dose rate brachytherapy source with analysis of statistical uncertainty. *Med Phys* 2006; 33: 163-172.
16. Dewerd LA, Ibbott GS, Meigooni AS et al. A dosimetric uncertainty analysis for photon-emitting brachytherapy sources: Report of AAPM Task Group no. 138 and GEC-ESTRO. *Med Phys* 2011; 38: 782-801.
17. Zourari K, Pantelis E, Karaiskos P et al. Clinical LDR prostate brachytherapy uncertainties from seed construction parameters. *Medical Physics International* 2013; 1: 236.
18. Rivard MJ, Butler WM, DeWerd LA et al. Supplement to the 2004 update of the AAPM Task Group No. 43 Report. *Med Phys* 2007; 34: 2187-2206.
19. Nunn AA, Davis SD, Micka JA et al. LiF:Mg,Ti TLD response as a function of photon energy for moderately filtered x-ray spectra in the range of 20-250 kVp relative to ^{60}Co. *Med Phys* 2008; 35: 1859-1869.
20. Rasmussen BE, Davis SD, Micka JA et al. Response of LiF:Mg,Ti thermoluminescent dosimeters to low-energy photons. *Med Phys* 2008; 35: 2792-2792.
21. Williamson JF. Monte Carlo modeling of the transverse-axis dose distribution of the Model 200 ^{103}Pd interstitial brachytherapy source. *Med Phys* 2000; 27: 643-654.
22. Williamson JF. Dosimetric characteristics of the DRAXIMAGE model LS-1 I-125 interstitial brachytherapy source design: A Monte Carlo investigation. *Med Phys* 2002; 29: 509-521.
23. Williamson JF. Comparison of measured and calculated dose rates in water near I-125 and Ir-192 seeds. *Med Phys* 1991; 18: 776-786.
24. Williamson JF, Coursey BM, DeWerd LA et al. Dosimetric prerequisites for routine clinical use of new low energy photon interstitial brachytherapy sources. *Med Phys* 1998; 25: 2269-2270.
25. Joint AAPM/RPC Registry of Brachytherapy Sources Meeting the AAPM Dosimetric Prerequisites, available online at: http://rpc.mdanderson.org/rpc/BrachySeeds/Source_Registry.htm (last accessed November, 27 2013).